

1 **From motor protein to toxin: Mutations in the zonula occludens toxin (Zot) of *Vibrio cholerae***
2 **phage CTX ϕ suggest a loss of phage assembly function**

3

4 Long Ma^{#1}, Simon Roux², Xiaoting Hua^{3,4}, Yong Wang⁵, Belinda Loh^{*#6}, and Sebastian Leptihn^{*1,3,7}

5 ¹ Zhejiang University-University of Edinburgh (ZJU-UoE) Institute, Zhejiang University, International
6 Campus, Haining, Zhejiang 314400, PR China

7 ² DOE Joint Genome Institute, Berkeley, CA, USA

8 ³ Department of Infectious Diseases, Sir Run Run Shaw Hospital, Zhejiang University School of
9 Medicine, Hangzhou, PR China

10 ⁴ Key Laboratory of Microbial Technology and Bioinformatics of Zhejiang Province, Hangzhou, China.

11 ⁵ The Provincial International Science and Technology Cooperation Base on Engineering Biology,
12 International Campus of Zhejiang University, College of Life Sciences, Shanghai Institute for Advanced
13 Study, Institute of Quantitative Biology, Zhejiang University, Haining 314400, China

14 ⁶ Department of Vaccines and Infection Models, Fraunhofer Institute for Cell Therapy & Immunology
15 (IZI), Perlickstr. 1, Leipzig, 04103, Germany.

16 ⁷ University of Edinburgh Medical School, Biomedical Sciences, College of Medicine & Veterinary
17 Medicine, The University of Edinburgh, 1 George Square, Edinburgh, EH8 9JZ, United Kingdom

18 # These authors contributed equally

19 *Corresponding authors:

20 Dr. Belinda Loh, E-mail: belinda.loh@izi.fraunhofer.de

21 Fraunhofer Institute for Cell Therapy & Immunology (IZI), Department of Vaccines and Infection Models,
22 Head of Antimicrobial Biotechnology, Perlickstr. 1, Leipzig, 04103, Germany.

23 Prof. Sebastian Leptihn, sebastian.leptihn@ed.ac.uk

24 Infection Medicine, Biomedical Sciences, Edinburgh Medical School, College of Medicine and
25 Veterinary Medicine, The University of Edinburgh, 47 Little France Crescent, EH16 4TJ Edinburgh,
26 United Kingdom

27

28 Running Title: Non-functional Walker motifs in *Vibrio cholerae* Zot

29 **Abstract**

30 Prophages, i.e. dormant viruses residing in bacterial cells, are not just passive passengers in the
31 bacterial host. Several prophage-encoded genes have been shown to be contributors to bacterial
32 virulence by mediating antimicrobial resistance or by providing toxins. Other prophage genes exhibit
33 beneficial effects on the host by modulating e.g. motility or biofilm formation. In this study, we used an
34 *in vivo* phage assembly assay and tested an extensive array of single point mutations or their
35 combinations found in Zot, the zonula occludens toxin encoded by the *Vibrio cholerae* phage CTX ϕ . The
36 assay makes use of the highly homologous Zot-like protein g1p of the filamentous Coliphage M13, a
37 motor protein that mediates the trans-envelope assembly and secretion of filamentous phages. We also
38 measured the *in vitro* ATP hydrolysis of purified proteins, and quantified virus production in *V. cholerae*
39 mediated by Zot or the Zot-like protein of the two *Vibrio* phages CTX ϕ and VFJ ϕ . In addition, we
40 investigated sequence variations of the Walker motifs in *Vibrio* species using bioinformatics method,
41 and revealed the molecular basis of ATP binding using molecular docking and molecular dynamics
42 simulation based on the structure predicted by AlphaFold2. Our data indicates that g1p proteins in *Vibrio*
43 can easily accumulate deleterious mutations and likely lose the ability to efficiently hydrolyse ATP, while
44 the CTX ϕ Zot was further exapted to now act as an auxiliary toxin during the infection by *Vibrio cholerae*.

45

46 **Keywords:** filamentous phage, CTX ϕ , Walker motifs, phage assembly, zonula occludens toxin (Zot),
47 g1p, ATPase

48

49

50

51 **Introduction**

52 Prophages, which exist in a “dormant” state until activation and initiation of replication, can have a
53 substantial impact on the host. A small minority of prophage-encoded genes are not directly required
54 for the viral replication cycle or genome insertion, nor do they encode for structural components of the
55 phage particle. Some of these “prophage accessory” genes have been identified as virulence factors
56 such as antimicrobial resistance genes or toxins. Prominent examples are the Shiga toxin- and the
57 Cholera toxin-encoding genes ¹⁻⁴. Other genes appear to influence bacterial host virulence indirectly by
58 e.g. inducing motility or biofilm formation. Similar to other prophages, filamentous phages, which lead
59 to a “chronic infection” with continuous viral replication while not killing the host, can play an important
60 role in the pathogenicity and fitness of their hosts ^{5,6}. While some inoviruses have been observed to
61 have a negative impact on fitness of infected bacteria, virulence factors that are transmitted via infection
62 by the virus or passed on vertically as a prophage, help the host to obtain an evolutionary advantage ⁷.
63 One of the best examples is the CTX ϕ phage infecting *Vibrio cholerae* that has been shown to be
64 responsible for transmitting the genes coding for the cholera toxin CTX to its host, rendering it highly
65 pathogenic in widespread cholera epidemics ⁸.

66

67 Filamentous phages are Inoviruses, single-stranded DNA viruses, with an extraordinary morphology
68 being essentially protein coated DNA filaments at approximately 1 μm in length and 6 nm in diameter ⁹.
69 In contrast to the head-and-tail phages, filamentous phages are less common and are often thought of
70 as an oddity among the prokaryotic viruses. However, they are found in almost all bacteria and possibly
71 also archaea ¹⁰, and particularly those in pathogens are of interest with regards to their contribution to
72 virulence of their hosts ^{6,11-13}. Filamentous phages are non-lytic and are extruded from the bacterial
73 envelope as the host continues to grow. After infecting their host, filamentous phages remain as an
74 episomal element or integrated into the genome while the phage DNA is being replicated and viral
75 particles are being produced, a “chronic infection”. The genomes of *Vibrio cholerae* contain a plethora
76 of prophages, including those of filamentous phages. Interestingly, according to a previous report, so
77 far not a single *V. cholerae* strain has been isolated that contains only a single chromosomally integrated
78 filamentous phage ¹⁴. For genome integration, a single dif site in *Vibrio cholerae* is used by several
79 phages including CTX ϕ and satellite phages RS1 ϕ and TLC ϕ ^{15,16}. The satellite phages RS1 ϕ and TLC ϕ

80 may require helper phages, as they do not encode morphogenesis proteins. In the case of RS1 ϕ , the
81 phages CTX ϕ or KSF-1 ϕ were proposed to mediate the encapsidation of the RS1 ϕ genome, similar to
82 TLC ϕ mediating the formation of fs2 ϕ viral particles¹⁷⁻²⁰.

83

84 The archetypical filamentous phages fd and M13 infect *E. coli*, with a genome that encodes only 11
85 genes, devoid of any virulence genes and only contain those responsible for replication or
86 morphogenesis. The products of five of these genes encode structural proteins that eventually cover
87 the DNA strand in the mature virion. The remaining six genes encode proteins that are involved in the
88 reproduction of genomic DNA in the host during the virus life cycle. Gene 1 is a phage-encoded gene
89 whose protein is essential for the assembly and extrusion of the phage, and is referred to as g1p, gp1
90 or p1. The protein is also called a Zot-like protein, as it is homologous to the *zonula occludens toxin* of
91 the filamentous *Vibrio cholerae* phage CTX ϕ . One of the key features of gene 1 (g1p) is that it contains
92 an internal ORF (gene 11, g11p) that has been shown to be necessary for phage production, and a
93 transmembrane domain that anchors the complex to the inner membrane of the host²¹. An essential
94 feature of gene 1 is the presence of Walker motifs which are the molecular basis for ATPase activity²².

95

96 Walker motifs are considered fundamental motifs in biological systems. Proteins found to possess
97 consensus Walker A motifs, A/GxxxxGKT/S (where x represents any amino acid) and consensus Walker
98 B motifs, hhhhDE (where h represents any hydrophobic residue) are highly likely to be functional
99 ATPases²³. Previous work conducted in our lab has shown that the putative Walker A and Walker B
100 motifs located at the N-terminus of g1p are required for the production of M13²². Sequence alignments
101 of gene 1 have shown that the Walker motifs are present across most species of filamentous phages.
102 A striking exception is found in the filamentous phage CTX ϕ , which infects *Vibrio cholera* and has been
103 shown to be responsible for the bacteria's pathogenicity, as it supplies the host with the phage-encoded
104 cholera toxin (CTX). The Walker motifs found in gene 1 of the CTX ϕ phage have mutations in key
105 positions in the consensus sequence that would theoretically render the protein inactive for ATPase
106 activity. The CTX ϕ protein Zot was investigated as one of two auxiliary toxins, in addition to CTX. Here,
107 the Zot protein was tested on human cells and was found to increase the permeability of small intestinal
108 mucosa by opening intercellular tight junctions^{24,25}.

109

110 In this work, we analysed the Zot/ Zot-like assembly genes of two filamentous *V. cholerae* phages and
111 compared it with the model phage M13. While the Walker motifs in *V. cholerae* phage VFJ ϕ has a
112 sequence in line with the consensus motif, CTX ϕ exhibits a deviant Walker A motif and an uncommon
113 Walker B motif, with bulky phenylalanine residues. Using a combination of protein biochemistry,
114 bioinformatics and *in vivo* methods, we could demonstrate that the Zot of CTX ϕ is highly inefficient in
115 ATP hydrolysis and phage assembly.

116

117

118 **Materials & Methods**

119 **Molecular biology.** Seamless cloning was used to generate plasmids; **Supplemental Table 1** lists
120 mutants and chimeras of gene 1 (UniProtKB: P03656) and ZOT/ZOT-like genes VFJX ϕ Zot (UniProtKB:
121 R9TFZ4) and CTX ϕ Zot (UniProtKB: P38442). QuikChange II site-directed mutagenesis was performed
122 according to the company's instructions (Agilent Technologies Inc., Santa Clara, CA, USA). The
123 numbering of amino acids follows the sequence of the M13 g1p.

124 ***In vivo* complementation assays (Spot tests).** Testing point mutations *in trans* was conducted as
125 previously described ²². Briefly, LB agar plates were top-layered with exponentially growing *E.coli*
126 expressing protein, mixed with LB agar (0.7% agar). Once the agar solidified, dilutions of the M13 phage
127 was then "spotted" and the plates were incubated at 37°C overnight to develop plaques. To quantify
128 phage titer, dilutions of the supernatant were mixed with *E. coli* mixed with LB agar (0.7% agar). After
129 incubating at 37°C overnight, plaques grown were counted, and the phage titer was calculated based
130 on the dilution factor.

131 **Quantification of viruses in bacterial culture supernatant.** To determine the exact amount of virus
132 particles assembled in the case of *V. cholerae* phage, we performed qPCR experiments as "spotting"
133 (described above) did not result in the formation of visible plaques-like zones. We designed three primer
134 pairs based on the receptor-binding proteins of the phages (called g3p, gp3 or p3) (**Supplemental Table**
135 **2**) allowing to correlate the amount of M13 phages detected in our *in vivo* assay, using spotting, with the
136 qPCR data. qPCR data was also correlated with the number of bacterial cells (to obtain phage
137 production values per host cell), determining the number of bacteria by qPCR using the 16S ribosomal
138 RNA gene (*rrsA*) ²⁶. The *V. cholerae* strain we used had the CTXb gene and ZOT genetically removed
139 from the CTX ϕ (kind gift from Prof. Menghua Yang, Zhejiang A & F University, Hangzhou, China). CTX ϕ
140 ZOT and the ZOT-like genes from VFJ ϕ were cloned into pBAD33 and chloramphenicol-resistant
141 colonies were selected after introduction of the respective plasmids by electroporation. Liquid cultures
142 were grown until an OD600 of 0.2 was reached, then 0.5 μ g/ml mitomycin C (final concentration) for
143 prophage induction and 0.2% L-Arabinose (final concentration) for plasmid-derived protein expression,
144 were added. After culturing for 4 hours, sedimentation and repeated washing, bacterial DNA was
145 extracted from 1 mL using the BMamp Rapid Bacteria DNA kit (Biomed, catalog number: DL111-01)
146 following the instruction manual. Next, we determined the number of phages in the supernatant. To 200

147 μL of supernatant 1 μL DNase (New England Biolabs, catalog number: M0303S) 1 μL RNaseA (Biomed,
148 catalog number: 756780AH) was added and incubated at 37 °C for 5 hours, followed by heat
149 denaturation at 70° C for 10 minutes to deactivate the enzymes. To remove proteins, 25 μL
150 proteinaseK was added followed by DNA extraction using the PureLink Viral RNA/DNA Mini Kit (Thermo
151 Fisher Scientific catalog number:12280050) according to the manufacturer's instructions. For the qPCR
152 we used the BlasTaq 2X qPCR MasterMix kit (Abm, catalog number: G891) in triplicates, with four
153 independent experiments.

154 **ATP Hydrolysis assay.** Expression and purification attempt of the entire genes were unsuccessful
155 either due to toxicity to the cells, expression level or inability to capture the protein on the column,
156 depending on the gene. Thus, only the ATPase domain containing cytoplasmic fragment of CTX ϕ ZOT
157 and the ZOT-like genes from VFJ ϕ were cloned into the *E. coli* expression vector pQE60 and expressed
158 at 20°C over night to obtain C-terminal MBP-fusion proteins in M15 cells. Protein purification was
159 performed with an AKTA pure system using MBPTrap HP 1ml column (Cytiva, catalog number:
160 28918778), protein concentration was determined via Bradford assay (Beyotime, catalog number:
161 P0006). EnzChek Phosphate Assay Kit (Thermo Fisher Scientific, catalog number: E6646) was used to
162 determine ATP hydrolysis rates according to the instructions provided by the manufacturer. After
163 establishing a phosphate standard curve, the assay was performed with different amounts of purified
164 proteins in triplicates with three independent repeats each using a newly expressed and purified protein
165 batch.

166 ***In silico* sequence analyses.** Phylogenetic Tree and sequence alignments were conducted using
167 Clustal Omega with the output using ClustalW alignment format ²⁷. Phylogenetic tree was visualised
168 using iTOL ²⁸.

169 **Structure prediction, molecular docking and molecular dynamics simulation.** AlphaFold (version
170 2.2) with default pipeline was used to predict the structures of M13-g1p, VFJ ϕ -Zot, and CTX ϕ -Zot. Five
171 structures were predicted for each protein and the top one was subsequently docked with an ATP
172 molecule in the cytoplasmic domain using AutoDock Vina ²⁹. For each complex, six docked models were
173 prepared.

174 The top ranked structure of the ATP-bound M13-g1p complex was embedded into a flat POPC lipid
175 bilayer and solvated in a cubic water box containing 0.15 M NaCl, using the "Membrane Builder" function

176 of the CHARMM-GUI webserver ³⁰. The OPM (Orientations of Proteins in Membranes) webserver was
177 used to align the transmembrane region (residue 254-270) in the lipid bilayer ³¹. The size of the
178 simulated box was 12.0 nm, 12.0 nm and 13.9 nm in the x, y and z dimension, respectively, resulting in
179 ~188,000 atoms in total. The CHARMM36m force field was used for the protein and the CHARMM36
180 lipid force field was used for the POPC molecules ³². ATP molecule was assigned with CHARMM
181 CGenFF force field. TIP3P model was used for the water molecules. The system was then energy
182 minimized and equilibrated in a stepwise manner using 1 ns NVT simulations and a following NPT
183 simulation. Finally, a 200 ns productive simulation was performed. Neighbor searching was performed
184 every 20 steps. Neighbor searching was performed every 20 steps. The PME algorithm was used for
185 electrostatic interactions with a cut-off of 1.2 nm. A reciprocal grid of 100 x 100 x 112 cells was used
186 with 4th order B-spline interpolation. A single cut-off of 1.2 nm was used for Van der Waals interactions.
187 The temperature was kept at 310 K with the V-rescale algorithms. The pressure was kept at 1.0×10^5
188 Pa with the Parrinello-Rahman algorithm. All simulations were performed using a GPU-accelerated
189 version of Gromacs 2021.5 ³³. Protein structures were visualized with PyMOL ³⁴.

190 **Identification of Walker sequences in *Vibrio* genomes.** 1,529 *Vibrio cholerae* genomes were
191 downloaded from NCBI RefSeq & GenBank databases (i.e. including potential redundancy) on June 28
192 2021 ³⁵. Hmsearch v ³⁶ was used to compare all proteins predicted in these genomes to the g1p-like
193 HMM profiles previously built from an extended catalog of inoviruses ³⁷. *Vibrio cholera* g1p-like proteins
194 were identified based on hits to these HMM profiles with a score ≥ 50 .
195

196 **Results**

197 *CTX ϕ Zot phylogenetic separation from homologs of other phages indicate a divergent evolutionary*
198 *pathway.*

199 While filamentous phages have mainly been found to infect Gram-negative bacteria, many have been
200 identified in the genomes of most bacterial families and archaea ³⁷. When analysing the amino acid
201 sequence of Zot from several characterised filamentous phages, the sequence clearly aligns with other
202 Zot or Zot-like proteins. However, several distinct features such as extended non-aligning stretches are
203 found in the Zot gene of phage CTX ϕ . The assembly proteins of M13 clusters with other proteins from
204 Enterobacteriaceae (e.g. *Salmonella enterica*, *Klebsiella pneumoniae*) but also with *Vibrio cholerae*
205 phage VFJ ϕ , while CTX ϕ Zot exhibits a larger evolutionary distance to the cluster (Figure 1A). This might
206 indicate that the sequence has undergone evolutionary changes and may have evolved to possibly
207 adopt a structure (and function) different from that of a phage assembly motor.

208

209 *Deviant Walker A and Walker B sequences in the CTX ϕ Zot nucleotide binding pocket*

210 The morphogenesis protein of the filamentous coliphage M13 consists of two parts, which are separated
211 by a transmembrane domain. The cytoplasmic domain contains a Walker A and a Walker B motif, while
212 the periplasmic domain is thought to form a continuous secretion tunnel together with the outer
213 membrane protein g4p or p4, allowing the assembled phage filament to cross the cell envelope (Figure
214 1B). When comparing the putative molecular motor protein complex of filamentous phages from different
215 species, we found that the Walker A and Walker B motifs do not necessarily follow the characteristic
216 amino acid consensus sequence (Supplemental Figure 1). Walker A, also known as the P- or phosphate
217 binding loop, frequently contains a leucine at position 10 (according to the g1p of the coliphage M13) in
218 most g1p homologues analysed. This allows a putative helix to form that, together with the beta-sheet
219 structure of the Walker B, allows the formation of a groove where ATP is able to bind prior to its
220 hydrolysis. Several sequences however, display a proline at this position instead, which creates a kink
221 in protein structures and is therefore helix-breaking. Somewhat surprising is the observation of a bulky
222 tyrosine residue in position 13 in the case of the protein from the *Vibrio cholerae* phage CTX ϕ . According
223 to the classical Walker A motif, this residue is occupied by a conserved glycine, the smallest and most
224 rotationally flexible residue, and no other amino acids have been reported so far (in all known ATPases,

225 not only viral ones). *V. cholerae* is the host for several filamentous phages, not exclusively CTX ϕ but
226 also a phage called VFJ ϕ . The Walker A and B sequences of this phage are almost identical to the one
227 from M13, with both, the P10 and the Y13 absent (Figure 1C). Walker B is described as four hydrophobic
228 residues followed by a D and E. In all g1p sequences of the studied phages we found this to be the
229 case. However, in the case of CTX ϕ , two phenylalanine residues are present in position 84 and 86.
230 Albeit hydrophobic, the 2 residues are considered rather bulky as the benzene group occupies a
231 comparably large space. In all other cases, the correlating residues are leucine, isoleucine or valine
232 residues.

233

234 *The introduction of deviant residues in Walker A and Walker B in M13 g1p abolished phage production*

235 To understand the impact of the residues we observed in the putative nucleotide binding regions in
236 CTX ϕ g1p, we conducted a series of *in vivo* tests where we mutated one residue at a time. In our *in vivo*
237 assay, phage production is assessed by making use of an amber mutant of phage M13 in which gene
238 1 is disrupted, unless it is present in a suppressor strain or complemented by a functional gene 1 *in*
239 *trans*. We previously showed that such a complementation by a plasmid-encoded gene 1 is possible
240 and allows the study of the impact of individual mutations in the gene ²². To investigate the impact of
241 the homologue sequences observed in CTX ϕ , we tested the complementation *in trans* for the individual
242 and combined mutations in M13 g1p. The replacement of the catalytic lysine residue in position 14
243 abolished phage production and served as a control ²². In contrast, the mutation of a lysine residue in
244 position 9 to an alanine had no impact on phage production (Figure 2A and B). However, replacing a
245 leucine in position 10 with the proline found in CTX ϕ g1p, reduced phage production to the same extent
246 as the replacement of the catalytic lysine did, with low numbers of phages being produced due to
247 reversion or translation errors. Similarly, mutating the glycine in position 13 to a tyrosine found in CTX ϕ ,
248 was not tolerated and almost no phages were produced. Also, combining mutations or replacing the
249 entire CTX ϕ -like Walker A motif in M13 g1p were unable to rescue the function of the protein.

250 We then investigated the role of the mutations in Walker B by replacing the corresponding residues in
251 M13 g1p with those found in CTX ϕ . Here, we observed that the introduction of one of the two
252 phenylalanine residues present in the *Vibrio* phage abolishes the function of the protein. While the L84F
253 mutation has no impact on the function of the protein, assessed by the production of phages, the

254 mutation V86F, resulted in a loss of function of g1p (Figure 2C and D). Again, combined mutations as
255 well as the replacement of the entire Walker B -from M13 to CTX ϕ - did not restore the function of the
256 protein.

257 As Walker A and Walker B form a binding pocket for ATP in ATPases, we also investigated the mutations
258 found in CTX ϕ by introducing them into both motifs in M13 g1p and determined if they were able to
259 restore protein function. Here we observed a severe reduction in the number of phages, indicating that
260 the mutated protein is rendered non-functional by the amino acid substitutions (Figure 2E and F). As *V.*
261 *cholerae* is the host of several filamentous phages, we questioned whether the gene1 homologue from
262 *Vibrio cholerae* phage VFJ ϕ has a functional ATPase. To this end, we mutated both motifs in M13 g1p
263 to the sequence found in VFJ ϕ and found that phage titres were unaffected regardless of the mutations
264 made in individual motifs or combined, indicating that bacteriophage VFJ ϕ has a functional ATPase in
265 the gene1 homologue (Figure 2E and F).

266

267 *VFJ ϕ Zot is able to mediate CTX ϕ phage assembly in Vibrio cholerae*

268 Since *V. cholerae* is the host of several filamentous phages and we found that VFJ ϕ -Zot encodes a
269 functional ATPase *in vivo*, we asked whether it was possible for VFJ ϕ -Zot to mediate the assembly of
270 CTX ϕ . In order to address this question, we first established the assay to study VFJ ϕ and CTX ϕ *in vivo*
271 as the common method of determining plaque forming units by counting plaques is not a reliable
272 approach here; phages VFJ ϕ and CTX ϕ were previously shown to produce very few plaques and hence
273 the chosen method of detection was qPCR²⁶. In order to validate the qPCR approach for detecting
274 phages, we made use of M13. *Gene 3* coding for the receptor-binding protein g3p was used for
275 amplification and was found to correlate with the number of phages determined by counting PFUs on
276 bacterial culture plates (Supplementary Figure 2). As we also wanted to quantify the number of phages
277 produced per cell, we used a set of primers to detect the ribosomal 16S gene in *V. cholerae*, following
278 a previously established protocol²⁶.

279 We then conducted *in vivo* complementation assays using a *Vibrio cholerae* strain that contains the
280 CTX ϕ (but not the VFJ ϕ) prophage genome but has the cholera toxin and the Zot genes deleted by
281 genetic engineering (Δ Zot). The Zot gene from either VFJ ϕ or CTX ϕ were then cloned under the control
282 of an arabinose inducible promoter. As a negative control, the plasmid backbone that does not contain

283 any gene was used. The constructs were introduced into the *V. cholera* Δ Zot strain and the number of
284 phages produced was quantified by qPCR. Using this method, the number of amplicons in the presence
285 of CTX ϕ -Zot remained low as in the case of the control plasmid. However, when VFJ ϕ -Zot was
286 introduced into the *V. cholera* Δ ZOT strain, we were able to detect phages (Figure 3). Phage production
287 in our assay was comparably low possibly due to low prophage induction efficiency despite the presence
288 of the inducer mitomycin C. Regardless of the low number, our data supports the hypothesis that CTX ϕ -
289 Zot is an inefficient or inactive assembly protein and the CTX ϕ phage is able to “hijack” the protein from
290 phage VFJ ϕ for its assembly.

291

292 *A highly conserved glutamine in g1p homologs is not conserved in CTX ϕ but is essential for assembly*
293 When aligning sequences of g1p homologs from several organisms, including *Vibrio cholerae*,
294 *Escherichia coli*, *Acinetobacter baumannii*, *Neisseria meningitidis*, *Klebsiella pneumoniae* and others,
295 we found a single highly conserved residue in addition to the Walker motifs. Among all investigated
296 filamentous phage assembly proteins we found Q126 to be conserved, with the exception of the protein
297 in CTX ϕ ; here, a proline can be found in the corresponding position (Figure 4A). To test if Q126 can be
298 replaced by a proline or other residues, we created single point mutations and tested them in the M13
299 *in vivo* complementation assay. Our results show that in M13, g1p Q126P is not functional as is the
300 replacement of glutamine by asparagine, glutamic acid and lysine among many others (Figure 4B).
301 Surprisingly, the only mutation we found to be tolerated, was a replacement with methionine, which
302 shares the same length but not the same charge with glutamine. At present, the function of this residue
303 remains speculative.

304

305 *Structure prediction and molecular dynamics simulation indicate a regulatory role of Q126 for ATP*
306 *binding*

307 As the role of the glutamine (Q126) in the hydrolysis of ATP by functional assembly proteins is unclear,
308 we resorted to structural biology using AlphaFold2 to predict the structures of M13 g1p, VFJ ϕ -Zot and
309 CTX ϕ -Zot. The predicted structures show that M13 g1p, VFJ ϕ -Zot and CTX ϕ -Zot share a similar
310 topology (Figure 5A). The cytoplasmic domains among the 3 proteins are highly similar however, CTX ϕ -

311 Zot is slightly more distinct from M13 g1p and VFJ ϕ -Zot, as indicated by the root mean squared
312 deviations (RMSD) of VFJ ϕ -Zot and CTX ϕ -Zot from M13 g1p (0.1 nm and 0.38 nm, respectively).
313 Interestingly, in the predicted structure of M13 g1p, Q126 is positioned in close proximity to the ATP-
314 binding pocket (Figure 5B). We speculated that Q126 may play an active role in ATP binding and release
315 in regulating phosphate hydrolysis. To test this hypothesis, we performed molecular docking on the
316 groove formed by residues from the Walker motifs and also all-atom molecular dynamics (MD)
317 simulation of M13 g1p based on the docked structures. In the MD simulation, we indeed observed that
318 Q126 could form extensive hydrogen bonding interactions with the nucleotide (Figure 5B and Movie in
319 SI), thus supporting a crucial role in regulating ATP hydrolysis. This may also explain why mutations are
320 not well tolerated in the protein including the proline residue found in the corresponding position of Q126
321 in CTX ϕ -Zot. Interestingly, in the structures, we observed a similar groove in all three proteins allowing
322 the binding of ATP molecules, assessed by molecular docking. However, the binding modes of ATP in
323 CTX ϕ Zot are distinctly different from M13 g1p and VFJ ϕ Zot. Aside from Q126, we also observed other
324 residues, such as S12, G13, K14, T15 in Walker A motif and R148, H175, T206, K207 in the loop region,
325 to form stable interactions with ATP, suggesting that they may contribute to ATP binding (Supplementary
326 Figure 3).

327

328 *The cytoplasmic domain of VFJ ϕ -Zot is able to hydrolyse ATP in vitro, while CTX ϕ -Zot shows no activity*
329 To test if the CTX ϕ -Zot or VFJ ϕ -Zot proteins show ATPase activity *in vitro*, we cloned and expressed
330 the cytoplasmic domains as MBP-fusion proteins in *E. coli* and purified them to homogeneity. The
331 proteins were then tested for their ability to hydrolyse the nucleotide *in vitro* in an absorbance-based
332 assay. While the Zot-like protein from VFJ ϕ clearly showed ATPase activity in a concentration
333 dependent manner, we were unable to detect any ATP hydrolysis in the case of the CTX ϕ -Zot protein
334 (Figure 5C and Supplementary Figure 4). However, often additional molecules such as substrate or co-
335 factors are required for proteins to show (full) activity if they are tightly controlled. With this caveat in
336 mind, the lack of activity of CTX ϕ -Zot in our assay indicates that the protein might be an inefficient
337 ATPase, or one that has lost its ability to hydrolyse ATP entirely.

338

339 *Divergence of Walker motifs in Vibrio genomes indicate that the CTX ϕ Zot-like Walker sequences are*
340 *prevalent in Vibrio cholerae but not in other Vibrio species.* Using previously developed HMM profiles ³⁷,
341 we identified 1,203 g1p-like proteins across 1,122 genomes of *Vibrio cholerae*. After aligning these
342 proteins, we could categorise the proteins into three main "variants", i.e. combinations of mutations: (1)
343 The CTX-like, containing three non-functional mutations in the Walker motifs and a Q126P mutation, (2)
344 the functional M13/VFJ-like including a Q126 residue, and (3) a "hybrid" category which contains one
345 deleterious mutation in the Walker A or B motif and the Q126P mutation. One more category called
346 "atypical" includes all other proteins that were detected by the algorithm with partially large variations in
347 sequence. Here, in some instances the Walker A follows the GxxxxGKT/S consensus, yet with a proline
348 in position 10 (47% of the "atypical" sequences). Others do not conform with the consensus motif albeit
349 the catalytic lysine residue is present. Most of the proteins in *Vibrio cholerae* are CTX ϕ -like (842) or
350 hybrid (263), and only 9 were clearly M13/VFJ ϕ -like, while the remaining 89 were g1p candidates with
351 atypical mutations ([Supplemental table 3](#)).

352 When analyzing putative filamentous prophages in *Vibrio sp.* excluding *V. cholerae*, we found that 1,607,
353 of 5,117 (~26%) contained M13/VFJ ϕ -like sequences, while only 7 displayed a combination of mutations
354 strictly identical to CTX (0.001%). These were all found in the *Vibrio mimicus* species, which is known
355 to sometimes encode cholera-like toxins ³⁸. However, a number of pl-like proteins found in other vibrio
356 species than *V. cholera* included some, but not all, of the CTX-like deleterious mutations. For instance,
357 we observed 187 instances of L10P, 5,143 instances of G13Y, 112 instances of V86F, and 3,731
358 instances of Q126P. This suggests that pl-like ATPases in *Vibrio* can accumulate deleterious mutations
359 relatively easily, most likely because of the possibility of complementation by an intact pl-like ATPase
360 from a co-infecting filamentous phage.

361

362

363 Discussion

364 *Vibrio cholerae* is the host for many phages and several of them are filamentous^{16,39-42}. In this work
365 we studied the Zonula occludens toxin (Zot) of the *Vibrio cholerae* phages VFJ ϕ and CTX ϕ and
366 compared it to the highly homologous filamentous phage assembly protein found in M13. CTX ϕ is well
367 known for its potential for toxigenic conversion, i.e. the conversion of *Vibrio cholerae* strains into virulent
368 ones that express the phage-encoded cholera toxin, making them more pathogenic. This phage has
369 been shown to encode additional toxins, one of which is Zot. Zot has been reported to create lesions in
370 tissue, specifically in the *zonlula occludens*, when investigating *V. cholerae* culture supernatants or the
371 recombinant protein Zot^{25,43,44}.

372 Zot contains regions that align with high homology to the assembly (or morphogenesis) protein g1p
373 of the coliphage M13, also known as p1, pl, g1p. Our previous work on the gene1 encoded assembly
374 complex of the coliphage M13 demonstrated that both Walker motifs are essential for phage assembly
375²². Making use of this system, we tested the deviant motifs found in CTX ϕ in our *in vivo* assay.

376 While Walker A and Walker B motifs remain identifiable when aligning related sequences to each
377 other, Walker A variants have been identified by aligning the large terminase proteins of lytic
378 bacteriophages⁴⁵. However, the consensus sequence for Walker A can be defined as S/GxxxxGKT/S
379 (with x being any residue). In our study, a deviation from the classical Walker A motif seems apparent:
380 A small and flexible glycine residue in position 13 (numbering according to g1p of M13) preceding the
381 catalytic lysine, present in all Walker A motifs reported thus far, is replaced by the large, aromatic side
382 chain of a tyrosine in CTX ϕ Zot. In addition, a helix-breaking proline is found in position 10 where a
383 leucine is found in most g1p homologs. In Walker B of CTX ϕ Zot, two phenylalanine residues are found
384 where more commonly less bulky hydrophobic residues are present, which precede the characteristic
385 DE dyad found in the motif. Our extensive set of experiments including single point mutations, their
386 combination and also domain swapping experiments of the protein from CTX ϕ (data not shown), indicate
387 that CTX ϕ Zot is not a functional ATPase. Hence, we propose that in order to produce CTX ϕ phage
388 particles, a co-infection with a second filamentous phage -such as VFJ ϕ - is required. This might allow
389 CTX ϕ to exploit the assembly complex from another phage, a phenomenon reported for other phages
390¹⁴. A major discrepancy between our finding and a previous report is the publication by Faruque, S.M.
391 et al. (2002), describing the biogenesis of filamentous phage particles found in *Vibrio cholerae*. The

392 authors stipulate that the genetic element RS1 which can be encapsidated into a filamentous phage
393 particle, requires another phage ¹⁷. RS1 itself does not code for any morphogenesis or coat proteins
394 and thus would rely on a phage with functional genes, including g1p. While the experimental evidence
395 is extensive and the conclusion of the publication sound, no whole genome sequence of the tested
396 bacterial strains is available, which allows the possibility that a second filamentous phage genome may
397 be present in the tested isolates.

398 To explore the question of whether a “borrowed” assembly protein could facilitate producing phage
399 particles, we made use of a strain that contains only one filamentous phage, CTX ϕ , in which the Zot
400 protein has been genetically removed. We determined the number of phage particles produced in the
401 strain when complemented with the Zot gene *in trans*, or the Zot-like gene from VFG ϕ which is highly
402 similar to the assembly gene from M13. While induction and viral production conditions in this plasmid
403 complementation experiments might not be optimal, we could establish that no phage particles were
404 produced when the CTX ϕ ZOT gene was introduced on a plasmid into the host, similar to the “empty”
405 control plasmid. In contrast, a plasmid encoding the VFJ ϕ ZOT-like gene resulted in the production of
406 phage particles albeit at a low number, indicating that the expressed protein has the ability to
407 encapsidate the DNA of CTX ϕ by assembling the coat proteins of the virus around the genome.

408 The ATPase activity we show here is the first demonstration of such activity in an *in vitro* assay
409 using the purified Zot protein. A previous attempt conducted by Schmidt et al. ⁴⁴ obtained purified protein
410 by denaturing the polypeptide using a chaotropic agent (guanidine HCl), which leads to protein unfolding
411 and the spontaneous refolding in physiological buffers is not guaranteed. Especially for kinases and
412 ATPases, refolding from denatured proteins can be challenging as often molecular chaperones are
413 required for folding ²⁷. To address the question of whether the proteins from the two *Vibrio* phages have
414 the ability to hydrolyse ATP, we purified the cytoplasmic domains of the proteins from both phages as
415 MBP-fusion proteins, as the full length proteins could not be captured on the column or showed toxicity
416 towards *E. coli* during expression. Consistent with the previously reported study by Schmidt et al, the
417 ATPase domain of CTX ϕ Zot shows no ATPase activity. However, the corresponding domain from the
418 VFJ ϕ phage clearly has the ability to hydrolyse the nucleotide. The observed hydrolysis rate of the
419 protein is not extensive compared to the control, the enzyme apyrase, possibly due to being tightly
420 controlled by co-factors such as host- and viral proteins, and the phage DNA. The *in vitro* assay using

421 the purified proteins provides additional evidence to hypothesize that CTX ϕ Zot is a protein that has
422 gained another, possibly more important, function during evolution. As the phage might be able to be
423 propagated by using another phage's assembly complex (as established for other filamentous phages),
424 the CTX ϕ Zot could develop to become a secondary toxin in addition to the cholera toxin CTX. Additional
425 evidence that CTX ϕ Zot may have evolved "away" from a motor protein to become a toxin is the
426 sequence that the protein displays in the periplasmic region in case of M13 g1p and other filamentous
427 phages. Here, the sequence appears to have almost no homology and little structural similarity
428 (Supplementary Figure 1).

429 If CTX ϕ has a dysfunctional motor protein (yet a functional accessory toxin), how does the virus
430 replicate? According to a previous study *Vibrio* strains often contain more than one filamentous phage
431 type, which would allow them to exploit the assembly machine of other phages. As the report was
432 published in 2011, we employed a recently established algorithm by Simon Roux et al ³⁷, to analyse
433 how many filamentous prophages are present per genome in *V. cholerae* strains. We found that ~68%
434 (n = 1,040) contain one filamentous prophage and 4% (n = 66) have two or more prophages, while none
435 could be detected in 423 of 1,529 (~28%) strains (Supplementary Figure 4B). While this is significantly
436 more than the 45% reported in a recent study which however analysed the sequences of all *Vibrio*
437 species for Inoviridae prophage sequences ⁴¹, our findings also indicate that CTX ϕ would in most cases
438 not be transmitted horizontally, should our interpretation of the findings in this study be accurate.

439 Our analysis of *Vibrio cholera* genomes might suggest that the CTX ϕ -like protein has been
440 "domesticated" for use as a toxin and is probably not able to function as a pI-like protein for inovirus
441 assembly. Proteins encoding a "hybrid" sequence contain a tyrosine in Walker A where a glycine should
442 be present, which in our *in vivo* test model would result in a non-functional protein. At present, it is
443 unclear if such proteins are possibly coding for functional ATPases, which would be a novelty in the field
444 of understanding ATP-binding and hydrolysis mechanisms. However, during evolution prophages can
445 undergo genetic alterations rendering them non-functional and unable to generate functional phage
446 particles, while genes that provide an evolutionary advantage to the host such as toxins are more likely
447 to be conserved.

448 Indication that the proteins with "deviant motifs" might be able to bind ATP and possibly hydrolyse
449 the nucleotide is given by the AlphaFold2 structure prediction, molecular docking and all-atom MD

450 simulation. Although all three proteins, CTX ϕ -Zot, VFJ ϕ -Zot and M13-g1p, show a conserved ATP
451 binding pocket in a structurally similar cytoplasmic domain, the residue Q126 in M13-g1p, observed to
452 form extensive interactions with the nucleotide in the MD simulation ([Supplementary movie MD3](#)) is
453 replaced by a proline residue in the corresponding position in CTX ϕ -Zot. This mutation in CTX ϕ -Zot may
454 reduce the binding affinity with ATP by breaking the interactions, and therefore abolish ATP hydrolysis,
455 despite the overall structure still being conserved.

456

457 Based on the data we obtained from our *in vivo* tests, bioinformatic analyses and *in vitro* enzymatic
458 assays, we argue that the ZOT gene in *V. cholerae* phage CTX ϕ has evolutionarily lost its original
459 function, i.e. to facilitate the assembly of the phage particle in the membrane, and now fulfils the role of
460 an auxiliary toxin during the infection process for its host.

461

462

463 **Acknowledgments**

464 We would like to thank Prof. Menghua Yang (ZAFU, Hangzhou, China) for providing us with El Tor V.
465 *cholerae* strain C6706, and for her advice on working with the pathogen, for which we would like to thank
466 Prof. Julia Fritz-Steuber (University of Hohenheim, Germany) as well. This work was supported by a
467 grant from the National Natural Science Foundation of China (32011530116). And the simulations were
468 supported by Information Technology Center and State Key Lab of CAD&CG, Zhejiang University. The
469 work conducted by the U.S. Department of Energy Joint Genome Institute, a DOE Office of Science
470 User Facility, is supported under Contract No. DE-AC02-05CH11231.

471

472 **Author Contributions**

473 B.L. and S.L. conceived the study, B.L. and M.L. designed the experiments; M.L., B.L., X.H., S.R. and
474 S.L. performed the experiments or analysed the data; B.L prepared the figures; S.L. and B.L. wrote the
475 paper. All authors agreed to the final version of the manuscript.

476

477 **Conflicts of Interest**

478 The authors declare no conflict of interest. The founding sponsors had no role in the design of the study;
479 in the collection, analyses, or interpretation of data; in the writing of the manuscript, and in the decision
480 to publish the results.

481

482

483 **References**

- 484 1 Boyd, E. F. & Brussow, H. Common themes among bacteriophage-encoded virulence factors
485 and diversity among the bacteriophages involved. *Trends Microbiol* **10**, 521-529,
486 doi:10.1016/s0966-842x(02)02459-9 (2002).
- 487 2 Herold, S., Karch, H. & Schmidt, H. Shiga toxin-encoding bacteriophages--genomes in motion.
488 *Int J Med Microbiol* **294**, 115-121, doi:10.1016/j.ijmm.2004.06.023 (2004).
- 489 3 Tinsley, C. R., Bille, E. & Nassif, X. Bacteriophages and pathogenicity: more than just providing
490 a toxin? *Microbes Infect* **8**, 1365-1371, doi:10.1016/j.micinf.2005.12.013 (2006).
- 491 4 Jamet, A. *et al.* A widespread family of polymorphic toxins encoded by temperate phages. *BMC*
492 *Biol* **15**, 75, doi:10.1186/s12915-017-0415-1 (2017).
- 493 5 Loh, B., Kuhn, A. & Leptihn, S. The fascinating biology behind phage display: filamentous phage
494 assembly. *Mol Microbiol* **111**, 1132-1138, doi:10.1111/mmi.14187 (2019).
- 495 6 Sweere, J. M. *et al.* Bacteriophage trigger antiviral immunity and prevent clearance of bacterial
496 infection. *Science* **363**, doi:10.1126/science.aat9691 (2019).
- 497 7 Wendling, C. C., Refardt, D. & Hall, A. R. Fitness benefits to bacteria of carrying prophages and
498 prophage-encoded antibiotic-resistance genes peak in different environments. *Evolution* **75**,
499 515-528, doi:10.1111/evo.14153 (2021).
- 500 8 Waldor, M. K. & Mekalanos, J. J. Lysogenic conversion by a filamentous phage encoding
501 cholera toxin. *Science* **272**, 1910-1914, doi:10.1126/science.272.5270.1910 (1996).
- 502 9 Kuhn, A. & Leptihn, S. Helical and filamentous phages. (2019).
- 503 10 Roux, S. *et al.* Author Correction: Cryptic inoviruses revealed as pervasive in bacteria and
504 archaea across Earth's biomes. *Nat Microbiol* **5**, 527, doi:10.1038/s41564-020-0681-5 (2020).
- 505 11 Rice, S. A. *et al.* The biofilm life cycle and virulence of *Pseudomonas aeruginosa* are dependent
506 on a filamentous prophage. *ISME J* **3**, 271-282, doi:10.1038/ismej.2008.109 (2009).
- 507 12 Burgener, E. B. *et al.* Filamentous bacteriophages are associated with chronic *Pseudomonas*
508 lung infections and antibiotic resistance in cystic fibrosis. *Sci Transl Med* **11**,
509 doi:10.1126/scitranslmed.aau9748 (2019).
- 510 13 Shapiro, J. W. & Putonti, C. UPPhi phages, a new group of filamentous phages found in several
511 members of Enterobacteriales. *Virus Evol* **6**, veaa030, doi:10.1093/ve/veaa030 (2020).

- 512 14 Rakonjac, J., Bennett, N. J., Spagnuolo, J., Gagic, D. & Russel, M. Filamentous bacteriophage:
513 biology, phage display and nanotechnology applications. *Current issues in molecular biology*
514 **13**, 51-76 (2011).
- 515 15 Rubin, E. J., Lin, W., Mekalanos, J. J. & Waldor, M. K. Replication and integration of a *Vibrio*
516 *cholerae* cryptic plasmid linked to the CTX prophage. *Mol Microbiol* **28**, 1247-1254,
517 doi:10.1046/j.1365-2958.1998.00889.x (1998).
- 518 16 Davis, B. M., Moyer, K. E., Boyd, E. F. & Waldor, M. K. CTX prophages in classical biotype
519 *Vibrio cholerae*: functional phage genes but dysfunctional phage genomes. *J Bacteriol* **182**,
520 6992-6998, doi:10.1128/JB.182.24.6992-6998.2000 (2000).
- 521 17 Faruque, S. M. *et al.* RS1 element of *Vibrio cholerae* can propagate horizontally as a filamentous
522 phage exploiting the morphogenesis genes of CTXphi. *Infect Immun* **70**, 163-170,
523 doi:10.1128/IAI.70.1.163-170.2002 (2002).
- 524 18 Faruque, S. M. *et al.* CTXphi-independent production of the RS1 satellite phage by *Vibrio*
525 *cholerae*. *Proc Natl Acad Sci U S A* **100**, 1280-1285, doi:10.1073/pnas.0237385100 (2003).
- 526 19 Hassan, F., Kamruzzaman, M., Mekalanos, J. J. & Faruque, S. M. Satellite phage TLCphi
527 enables toxigenic conversion by CTX phage through dif site alteration. *Nature* **467**, 982-985,
528 doi:10.1038/nature09469 (2010).
- 529 20 Krupovic, M., Prangishvili, D., Hendrix, R. W. & Bamford, D. H. Genomics of bacterial and
530 archaeal viruses: dynamics within the prokaryotic virosphere. *Microbiol Mol Biol Rev* **75**, 610-
531 635, doi:10.1128/MMBR.00011-11 (2011).
- 532 21 Rapoza, M. P. & Webster, R. E. The products of gene I and the overlapping in-frame gene XI
533 are required for filamentous phage assembly. *J Mol Biol* **248**, 627-638,
534 doi:10.1006/jmbi.1995.0247 (1995).
- 535 22 Loh, B., Haase, M., Mueller, L., Kuhn, A. & Leptihn, S. The Transmembrane Morphogenesis
536 Protein gp1 of Filamentous Phages Contains Walker A and Walker B Motifs Essential for Phage
537 Assembly. *Viruses* **9**, doi:10.3390/v9040073 (2017).
- 538 23 Koonin, E. V., Tatusov, R. L. & Rudd, K. E. Sequence similarity analysis of *Escherichia coli*
539 proteins: functional and evolutionary implications. *Proc Natl Acad Sci U S A* **92**, 11921-11925,
540 doi:10.1073/pnas.92.25.11921 (1995).

- 541 24 Uzzau, S., Cappuccinelli, P. & Fasano, A. Expression of *Vibrio cholerae* zonula occludens toxin
542 and analysis of its subcellular localization. *Microb Pathog* **27**, 377-385,
543 doi:10.1006/mpat.1999.0312 (1999).
- 544 25 Di Pierro, M. *et al.* Zonula occludens toxin structure-function analysis. Identification of the
545 fragment biologically active on tight junctions and of the zonulin receptor binding domain. *J Biol*
546 *Chem* **276**, 19160-19165, doi:10.1074/jbc.M009674200 (2001).
- 547 26 Takahashi, N. *et al.* Lethality of MalE-LacZ hybrid protein shares mechanistic attributes with
548 oxidative component of antibiotic lethality. *Proc Natl Acad Sci U S A* **114**, 9164-9169,
549 doi:10.1073/pnas.1707466114 (2017).
- 550 27 Sievers, F. *et al.* Fast, scalable generation of high-quality protein multiple sequence alignments
551 using Clustal Omega. *Mol Syst Biol* **7**, 539, doi:10.1038/msb.2011.75 (2011).
- 552 28 Letunic, I. & Bork, P. Interactive Tree Of Life (iTOL) v5: an online tool for phylogenetic tree
553 display and annotation. *Nucleic Acids Res* **49**, W293-W296, doi:10.1093/nar/gkab301 (2021).
- 554 29 Trott, O. & Olson, A. J. AutoDock Vina: improving the speed and accuracy of docking with a
555 new scoring function, efficient optimization, and multithreading. *J Comput Chem* **31**, 455-461,
556 doi:10.1002/jcc.21334 (2010).
- 557 30 Jo, S., Kim, T., Iyer, V. G. & Im, W. CHARMM-GUI: a web-based graphical user interface for
558 CHARMM. *J Comput Chem* **29**, 1859-1865, doi:10.1002/jcc.20945 (2008).
- 559 31 Lomize, A. L., Pogozheva, I. D. & Mosberg, H. I. Anisotropic solvent model of the lipid bilayer.
560 1. Parameterization of long-range electrostatics and first solvation shell effects. *J Chem Inf*
561 *Model* **51**, 918-929, doi:10.1021/ci2000192 (2011).
- 562 32 Huang, J. *et al.* CHARMM36m: an improved force field for folded and intrinsically disordered
563 proteins. *Nat Methods* **14**, 71-73, doi:10.1038/nmeth.4067 (2017).
- 564 33 Abraham, M. J. *et al.* GROMACS: High performance molecular simulations through multi-level
565 parallelism from laptops to supercomputers. *SoftwareX* **1**, 19-25 (2015).
- 566 34 DeLano, W. L. Pymol: An open-source molecular graphics tool. *CCP4 Newsl. Protein*
567 *Crystallogr* **40**, 82-92 (2002).
- 568 35 Kitts, P. A. *et al.* Assembly: a resource for assembled genomes at NCBI. *Nucleic Acids Res* **44**,
569 D73-80, doi:10.1093/nar/gkv1226 (2016).

- 570 36 Eddy, S. R. Accelerated Profile HMM Searches. *PLoS Comput Biol* **7**, e1002195,
571 doi:10.1371/journal.pcbi.1002195 (2011).
- 572 37 Roux, S. *et al.* Cryptic inoviruses revealed as pervasive in bacteria and archaea across Earth's
573 biomes. *Nat Microbiol* **4**, 1895-1906, doi:10.1038/s41564-019-0510-x (2019).
- 574 38 Spira, W. M. & Fedorka-Cray, P. J. Purification of enterotoxins from *Vibrio mimicus* that appear
575 to be identical to cholera toxin. *Infect Immun* **45**, 679-684, doi:10.1128/iai.45.3.679-684.1984
576 (1984).
- 577 39 Campos, J. *et al.* VGJ phi, a novel filamentous phage of *Vibrio cholerae*, integrates into the
578 same chromosomal site as CTX phi. *J Bacteriol* **185**, 5685-5696, doi:10.1128/JB.185.19.5685-
579 5696.2003 (2003).
- 580 40 Canchaya, C., Proux, C., Fournous, G., Bruttin, A. & Brussow, H. Prophage genomics. *Microbiol*
581 *Mol Biol Rev* **67**, 238-276, table of contents, doi:10.1128/MMBR.67.2.238-276.2003 (2003).
- 582 41 Castillo, D. *et al.* Widespread distribution of prophage-encoded virulence factors in marine
583 *Vibrio* communities. *Sci Rep* **8**, 9973, doi:10.1038/s41598-018-28326-9 (2018).
- 584 42 Hay, I. D. & Lithgow, T. Filamentous phages: masters of a microbial sharing economy. *EMBO*
585 *Rep* **20**, doi:10.15252/embr.201847427 (2019).
- 586 43 Fasano, A. *et al.* *Vibrio cholerae* produces a second enterotoxin, which affects intestinal tight
587 junctions. *Proc Natl Acad Sci U S A* **88**, 5242-5246, doi:10.1073/pnas.88.12.5242 (1991).
- 588 44 Schmidt, E., Kelly, S. M. & van der Walle, C. F. Tight junction modulation and biochemical
589 characterisation of the zonula occludens toxin C-and N-termini. *FEBS Lett* **581**, 2974-2980,
590 doi:10.1016/j.febslet.2007.05.051 (2007).
- 591 45 Mitchell, M. S. & Rao, V. B. Novel and deviant Walker A ATP-binding motifs in bacteriophage
592 large terminase-DNA packaging proteins. *Virology* **321**, 217-221,
593 doi:10.1016/j.virol.2003.11.006 (2004).
- 594
- 595

596 **Figure Legends**

597 **Figure 1:** A) Circular phylogenetic tree comparing various Zot-like proteins from different organisms.

598 Sen-: *Salmonella enterica*; Kpn-: *Klebsiella pneumoniae*; M13-: *Escherichia virus M13*; Vha-:

599 *Virgibacillus halodenitrificans*; Ssa-: *Streptococcus sanguinis*; VFJ-: *Vibrio virus VFJφ*; Rto-:

600 *Ruminococcus torques*; Pf3-: *Pseudomonas virus Pf3*; Nmen-: *Neisseria meningitidis*; Ehm-:

601 *Enterobacter hormaechei*; Yen-: *Yersinia enterocolitica*; Ype-: *Yersinia pestis*; Aba-: *Acinetobacter*

602 *baumannii*; phiLf-: *Xanthomonas* phage phiLf; CTX-: *Vibrio virus CTXφ*. B) Schematic representation of

603 full length ZOT and ZOT-like proteins from M13, VFJφ and CTXφ. ZOT-like g1p in both M13 and VFJφ

604 contain an internal ORF which encodes gene 11. In CTXφ, the start of gene 11 and its function are less

605 clear. Purple box: Walker A motif. Blue box: Walker B motif. Arrow indicates internal open reading frame

606 of g1p1. TM: transmembrane region. C) Amino acid alignment of Walker A and Walker B motifs in the

607 ZOT protein of filamentous phages M13, VFJφ and CTXφ. Numbers above the alignment indicate amino

608 acid positions in M13 gene1. Consensus sequences are indicated below.

609

610 **Figure 2:** CTXφ Walker motifs result in dysfunctional protein. A & B) Residues in Walker A of M13

611 gene1 were mutated to CTXφ Walker A sequence and tested in *in vivo* complementation assays. C &

612 D) Residues in Walker B of M13 gene1 were mutated to CTXφ Walker B sequence and tested in *in vivo*

613 complementation assays. E & F) Residues in Walker A and B of M13 gene1 were mutated to VFJφ and

614 CTXφ Walker A and B sequence and tested in *in vivo* complementation assays. A,C,E) Amino acid

615 alignment of Walker motifs. Numbers above the alignment indicate amino acid positions in M13 gene1.

616 B,D,F) Phage titre from *in vivo* complementation assays with gene1 Walker motif mutants.

617

618 **Figure 3:** CTXφ-ZOT is dysfunctional *in vivo*. Expression of CTXφ-ZOT in *V. cholera* ΔZOT strain results

619 in as few phages produced as seen in control. Expression of VFJφ-ZOT facilitates phage production.

620 Control: Parent plasmid without ZOT gene.

621

622 **Figure 4:** Residue Q126 is important for protein function. A) Schematic representation of the M13 gene1

623 and homologues in VFJφ and CTXφ, with position of the Q residue included. B) Phage titre from *in vivo*

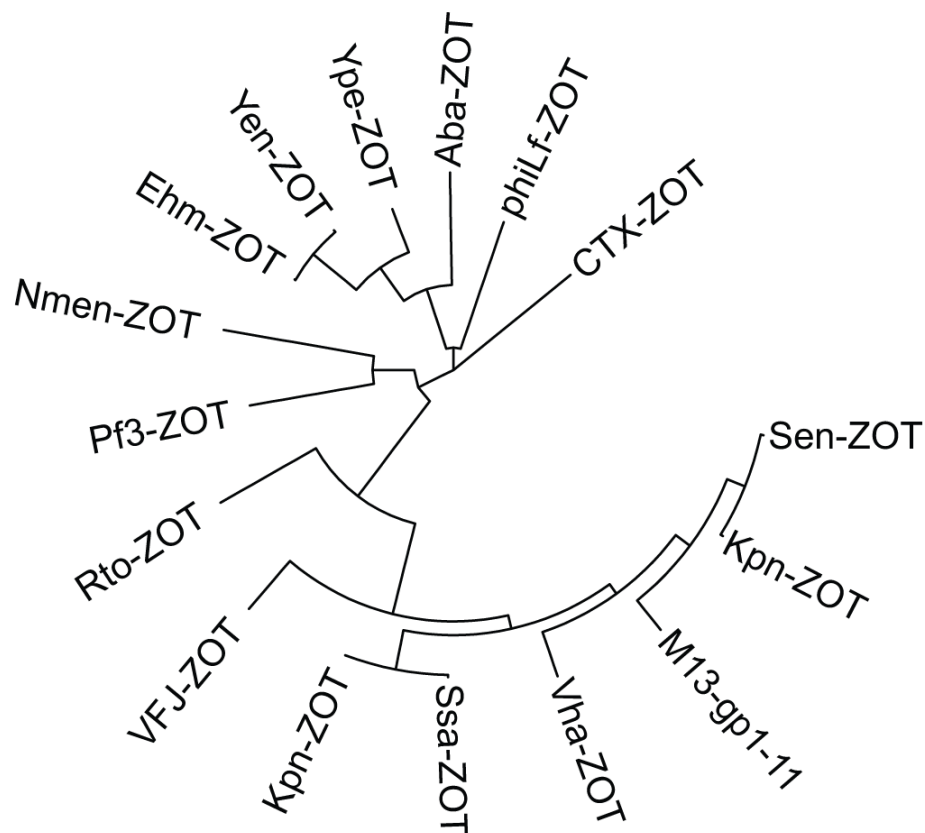
624 complementation assays with gene1 Q126 mutants.

625 **Figure 5:** Structures of M13-g1p, VFJ ϕ -Zot and CTX ϕ -Zot predicted by AlphaFold2. A) Five models
626 were predicted for each protein. The models are represented as cartoons coloured in blue to red from
627 the N-terminal region to the C-terminal region. B) Molecular docking of ATP within M13 g1p, VFJ ϕ Zot
628 and CTX ϕ Zot. The top six structures are represented. Note that different from M13 g1p and VFJ ϕ Zot,
629 the residue at the corresponding position of Q126 is P140 in CTX ϕ Zot.
630

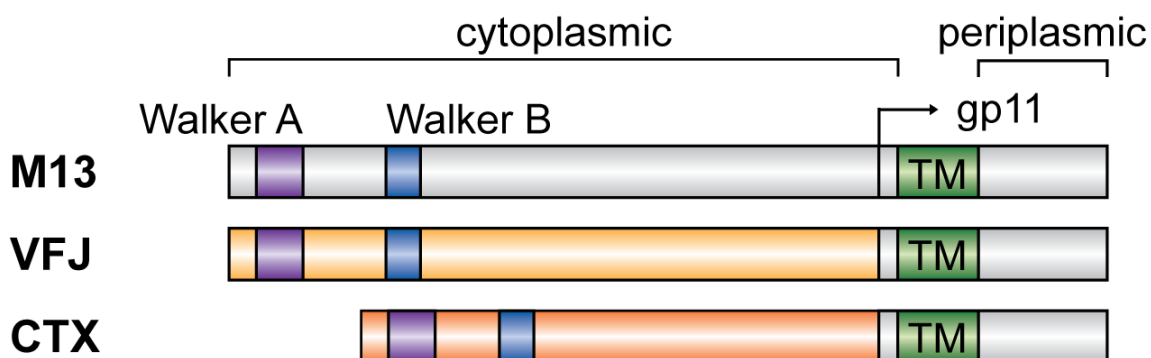
Figure 1

bioRxiv preprint doi: <https://doi.org/10.1101/2022.09.21.508815>; this version posted September 21, 2022. The copyright holder for this preprint (which was not certified by peer review) is the author/funder, who has granted bioRxiv a license to display the preprint in perpetuity. It is made available under aCC-BY-NC 4.0 International license.

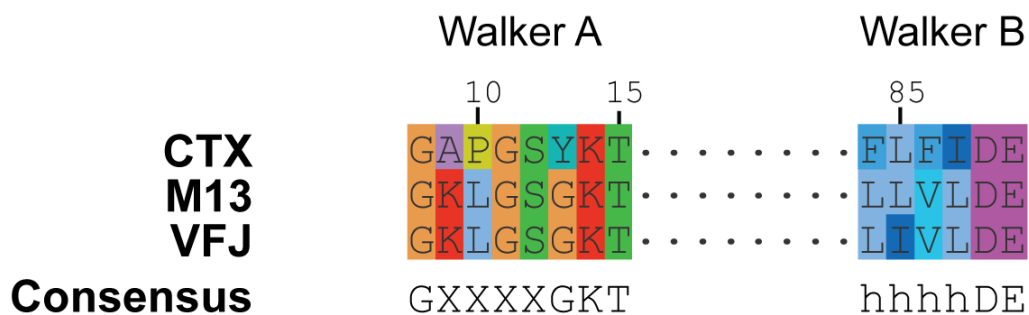
A



B

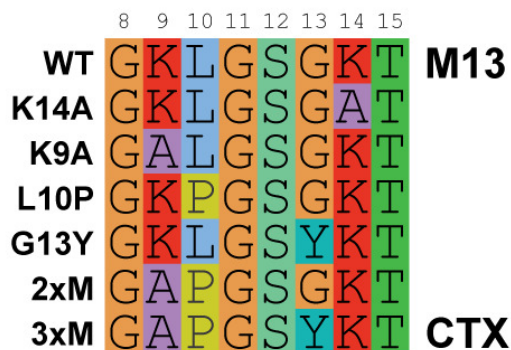


C

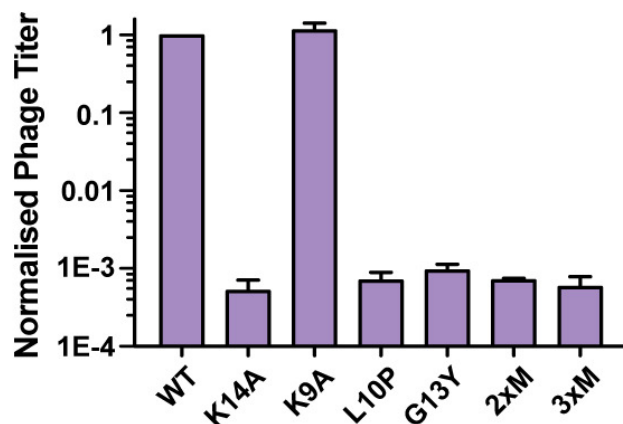


A

Walker A

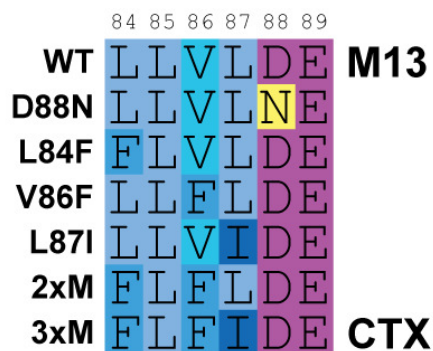


B

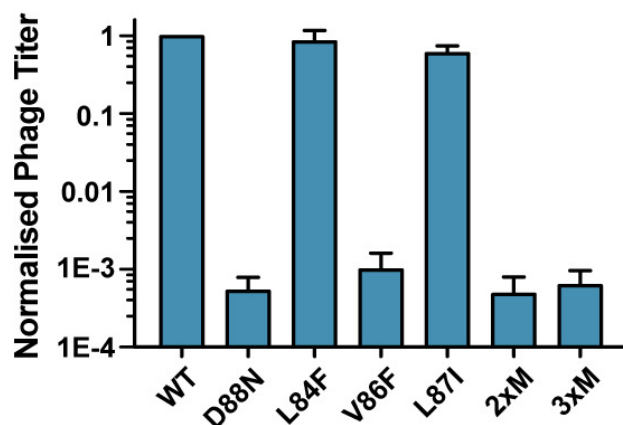


C

Walker B



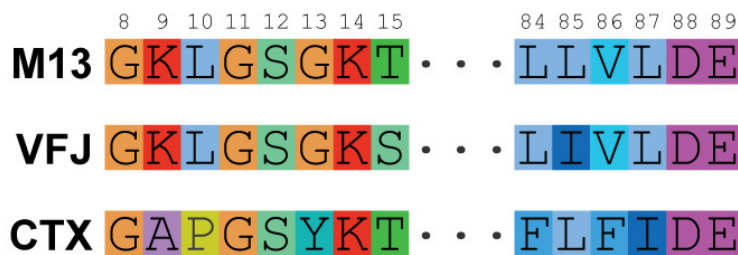
D



E

Walker A

Walker B



F

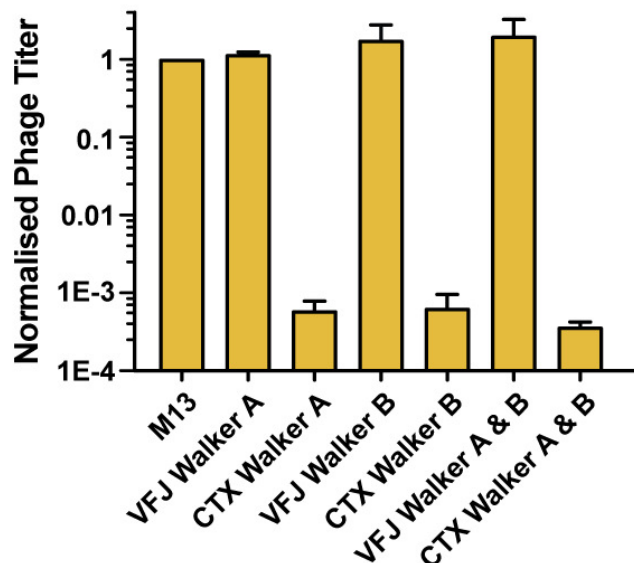


Figure 3

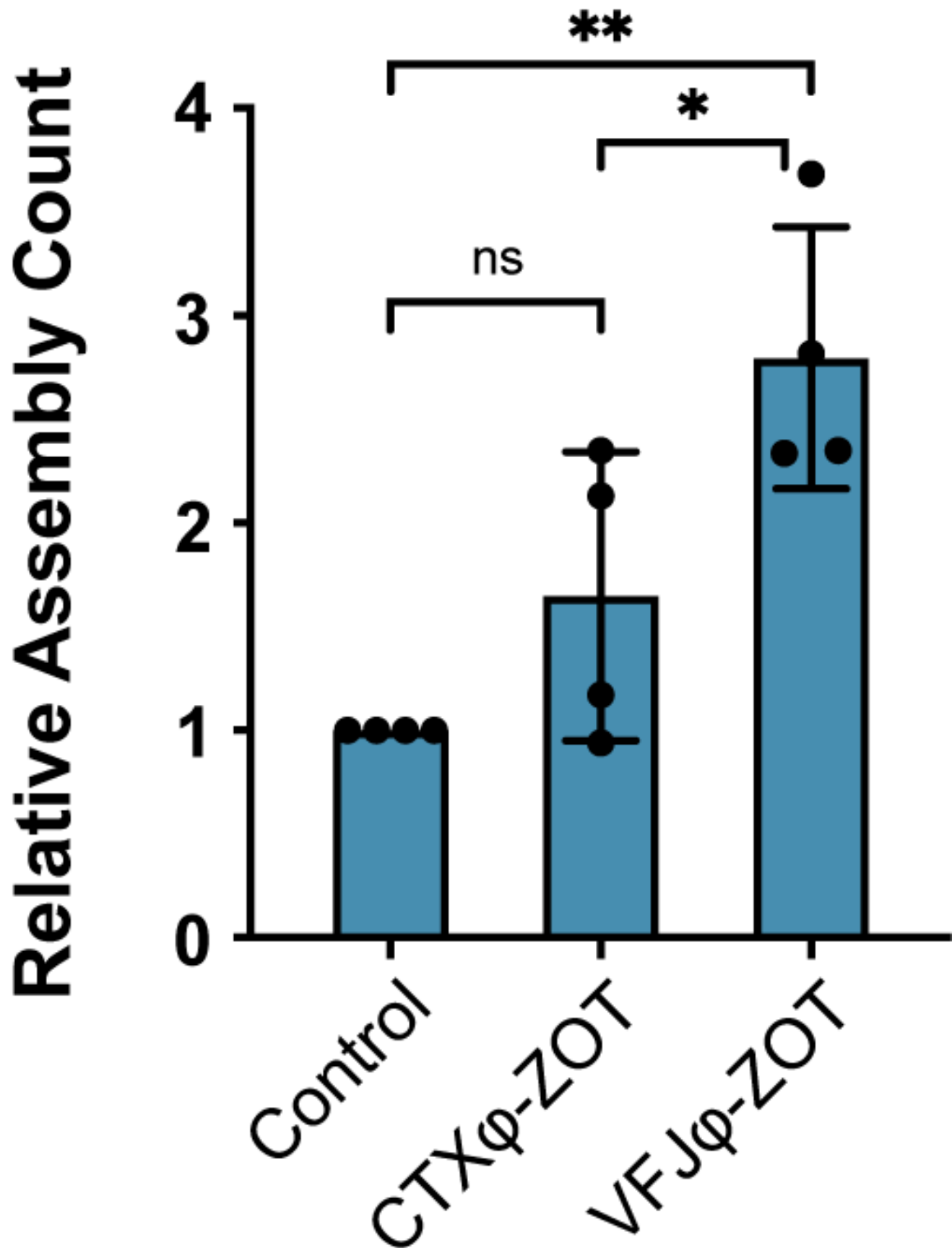
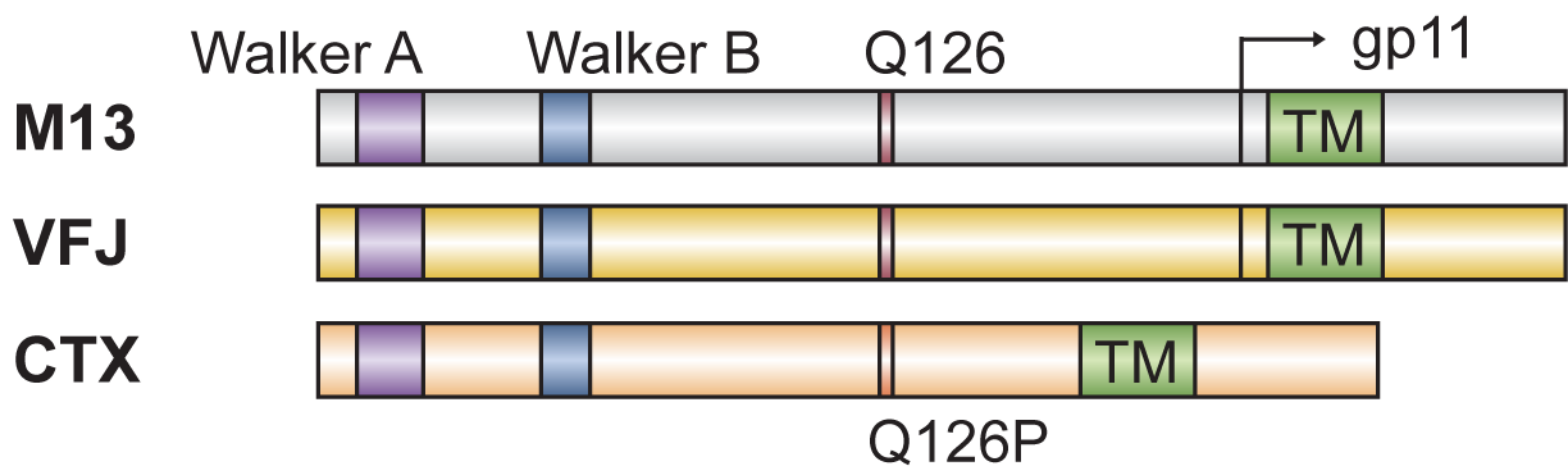
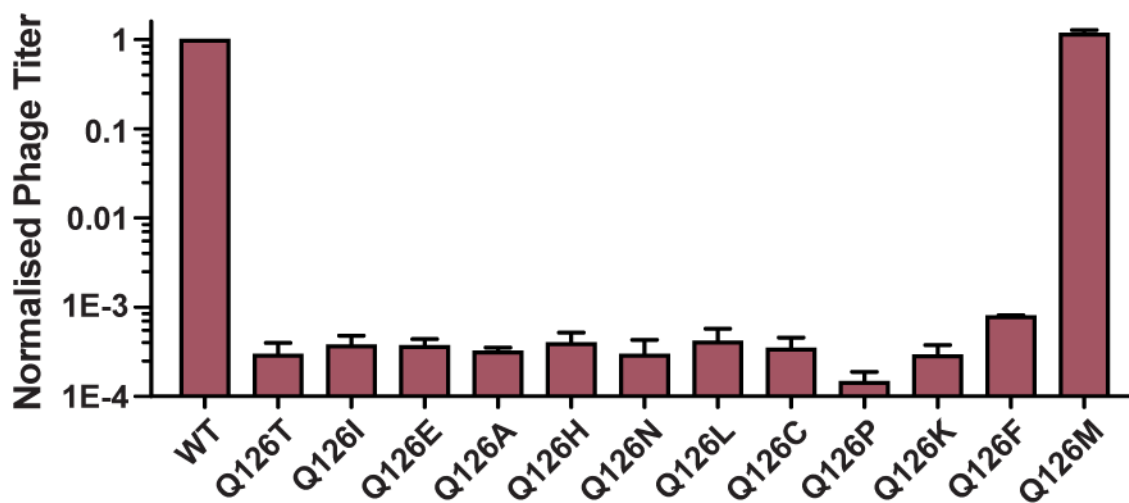


Figure 4

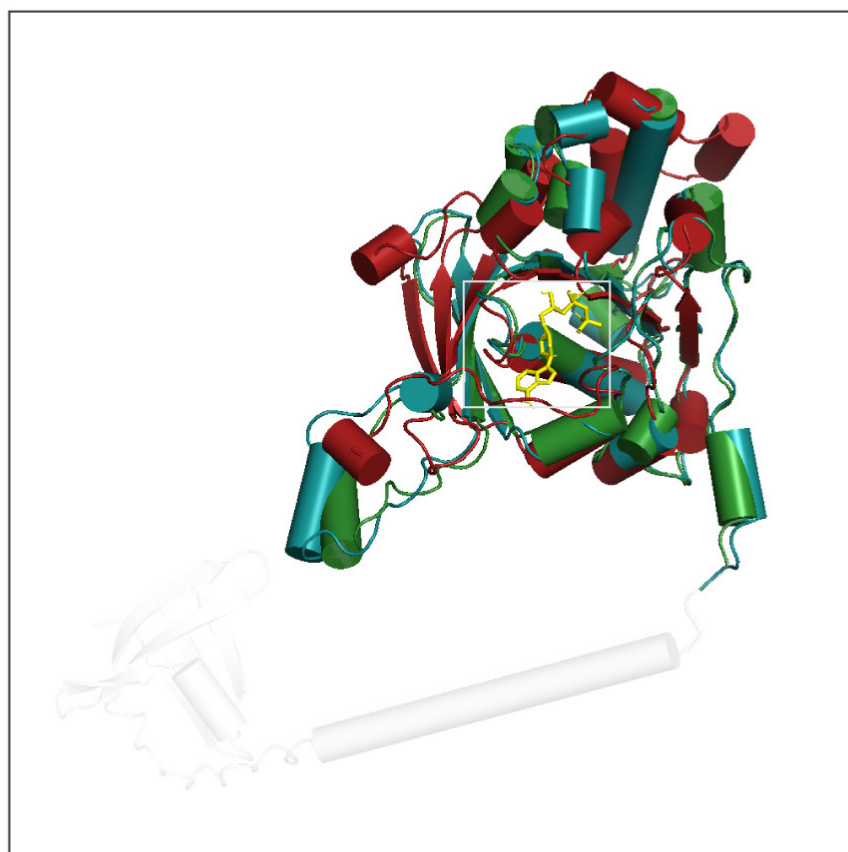
A



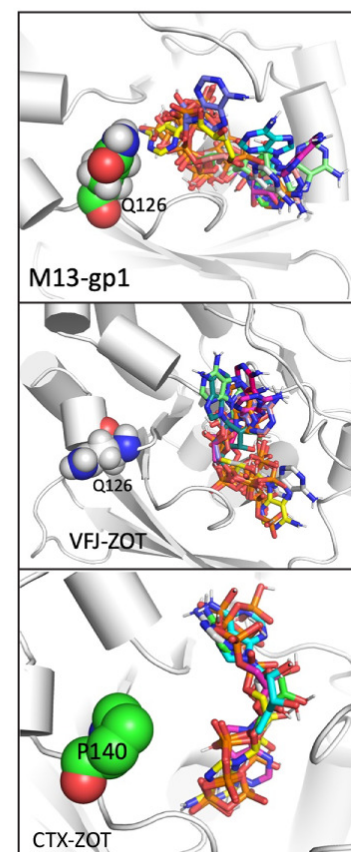
B



A



B



C

